Errors of In-Phase and Quadrature demodulation method created by low-pass filter

George P. Miroshnichenko[a], Alina N. Arzhanenkova[b], Michail Yu. Plotnikov[c]

ITMO University, St. Petersburg, Russia

[a]gpmirosh@gmail.com, [b]11arzh11@gmail.com, [c]plotnikov-michael@yandex.ru

Corresponding author: George P. Miroshnichenko, gpmirosh@gmail.com

ABSTRACT This article explores phase errors created by low-pass filter in interferometric signals which are processed by In-Phase and quadrature demodulation algorithm (IQ-demodulation). These errors were calculated using the analytical method and were compared with mathematical modeling, which uses pre-calculated parameters: phase, sampling period, infinitesimal parameters. In this paper, we show that phase errors calculated with analytical method clearly correlate with mathematical modeling errors. This work made it possible to calculate corrections to the demodulated phase, which, in turn, made it possible to refine the phase calculation step in IQ demodulation algorithm using the arctangent function. The resulting formulas describing the correction to the demodulated phase will increase the accuracy of the quadrature method, which is used to process signals from interferometric devices of various types, such as: reflectometers, geophysical seismic systems, interferometric radiometry, etc.

KEYWORDS demodulation, IQ demodulation, interferometry, measurement errors, sawtooth modulation

FOR CITATION Miroshnichenko G.P., Arzhanenkova A.N., Plotnikov M.Yu. Errors of In-Phase and Quadrature demodulation method created by low-pass filter. *Nanosystems: Phys. Chem. Math.*, 2024, **15** (3), 325–331.

1. Introduction

Fiber-optical interferometric sensors based on phase difference measurement in signal and control interferometer arms, which is created by the interaction of the fiber and environment. Mach–Zehnder, Michelson, Sagnac and Fabry–Perot interferometers are often used as sensors. It can also be "moving" interferometers, where interfering beams are Rayleigh scattering waves which were excited by a light pulse propagating in the fiber, as it happens, for example, in coherent reflectometry schemes. Optical circuits, which are used to measure phase shifts, implement three classical phase demodulation methods: Phase Generated Carrier (PGC) demodulation method, 3×3 coupler demodulation method, and In-phase and Quadrature (IQ) demodulation method [1]. Phase demodulation is used in many interferometric devices such as temperature and pressure sensors, fiber accelerometers and hydrophones, which are used in seismoacoustic streamers [2, 3].

Signal $S_{in}(t)$ taken from detector, value of the intensity of interfering waves, consists of two terms:

$$S_{in}(t) = F + G \cdot \cos(\omega t + \varphi(t)). \tag{1}$$

The first term, F, is the total intensity of the interfering waves, the second term is the interfering term which changes periodically with the modulation frequency ω and depends on the signal (measured) phase $\varphi(t)$. Parameter G determines so-called interference fringes visibility G/F.

Variable signal changed at high frequency ω and depends on slow-changed phase, which contains environment information. This method use two local oscillator signals which changed at frequency ω and shifted related to each other at $\pi/2$ radians in phase:

$$L_1(t) = I \cdot \cos(\omega t), \quad L_2(t) = I \cdot \sin(\omega t),$$

where I is the local oscillator intensity value.

Signals of local oscillators are multiplied with processed signal (1). As a result of applying low-frequency filters in this method, two low-frequency signals generate two quadratures: changing in phase (In-phase signal) and shifted by (Quadrature signal) signals

$$C(t) = G \cdot I \cdot \cos(\varphi(t)), \quad S(t) = G \cdot I \cdot \sin(\varphi(t)).$$

Subsequent processing of quadrature allows one to determine the phase and the amplitude of measured signal.

$$G \cdot I = \sqrt{S(t)^2 + C(t)^2}, \quad \varphi(t) = \arctan\left(\frac{S(t)}{C(t)}\right).$$

2. Previous researches

IQ demodulation scheme is the part, for example, of schemes for coherent phase-sensitive optical reflectometry of fiber optic channels in the time domain (Φ-OTDR). Phase demodulation of the backscattered light interference signal provides unique local information about the state of the optical fiber at distances of hundreds of kilometers. A balanced photodetector measures the temporal speckle of the interference. By monitoring the change in the speckle for successive injected pulses, one can detect a local change in the refractive index of the fiber under test. In a heterodyne detection system, an intermediate frequency signal, on the order of 200 MHz, at the output of a photon balanced detector, is acquired by a data acquisition system at a sampling rate several times that of the intermediate frequency, and digital In-phase/Quadrature (IQ) demodulation is performed to obtain phase information [2, 4–19]. In articles [2, 4, 5, 10], an optical IQ demodulation scheme instead of digital RF demodulation is presented. Here, a 90-degree optical hybrid is used to obtain the IQ components of the Rayleigh backscatter signal, which can significantly reduce computational costs. In [2], a heterodyne polling system for an array of interferometric fiber optic sensors with time multiplexing is used to demodulate the phase shift using the IQ demodulation method. The interference signal is generated in unbalanced Michelson interferometers. The method showed a high degree of linearity and a low level of noise. Heterodyne reception transfers the 1550.12 nm signal to the 200 MHz intermediate frequency region, where IQ method is used to extract the phase. Quadrature signal processing has a unique advantage in demodulating fiber Bragg grating interferometer sensors [2, 11, 15], which convert strain-induced changes in the Bragg wavelength into changes in intensity.

The quality of phase and amplitude reproduction depends on the noise level of the installation, among which, the main ones are: shot noise (depending on the dark current of the detector and on the receiver bandwidth), thermal noise (depending on the absolute temperature and load resistor) [10]. The articles [2, 4, 6–8, 11] analyze a possible drawback of the IQ demodulation method associated with inevitable hardware defects. This is an imbalance of quadrature amplitudes, which can manifest itself in both the DC and AC components of the received signals. An IQ imbalance can lead to signal distortion and reduced signal-to-noise ratio. In the listed works, a method for compensating for the imbalance was developed. As shown in [2], after compensation for the amplitude imbalance in the demodulated signals, there are still some internal distortions that arise due to the time skew and phase mismatch of the IQ signals. This article proposes a new method that takes into account the effects of high frequency cable length differences, fiber length differences, and non-orthogonality between IQ signals, providing a basis for accurate real-time compensation.

In this work, we neglect the noise characteristics in the signal $S_{in}(t)$, so signal $S_{in}(t)$ is written as follows:

$$S_{in}(t) = F + G \cdot \cos\left(\text{Saw}(t) + \varphi(t)\right). \tag{2}$$

After that, we explore corrections to quadrature signals $S(t)$, $C(t)$ from LPF. Here we used sawtooth phase modulation $\text{Saw}(t)$, which depends on time, with "saw" tilt Ω and period T_c.

3. LPF-moving average filter

Main characteristics of any non-recursive low-pass filter are frequency response, impulse response, and impulse response width [20]. Discrete moving average filter, which used in ADC (analog-to-digital converters), has the following impulse response:

$$y_n = \frac{1}{P} \cdot \sum_{j=n}^{n+P-1} x_j. \tag{3}$$

Here, P is the averaging interval (filter order), ω_d is the sampling frequency, ω_c is the modulation frequency.

$$P = \frac{\omega_d}{\omega_c} = \frac{T_c}{T_d}.$$

It should be remembered, that ω_c is always less than Nyquist frequency $\omega_d/2$. This condition means that $P > 2$. Here T_c is the modulation period, T_d is the sampling period. With this choice of filter order, we obtain the important relation

$$\sum_{j=n}^{n+P-1} \exp\left(i \cdot r \cdot \omega_c \cdot j \cdot T_d\right) = 0, \tag{4}$$

where r is an integer. Let's write formula (3) in continuous form, assuming that

$$y(t) = \frac{1}{T_c} \cdot \int_t^{t+T_c} x(t')\,dt'. \tag{5}$$

Feature (4) is true in continuous form:

$$\int_t^{t+T_c} \exp\left(i \cdot r \cdot \omega_c \cdot t'\right) dt' = 0.$$

Apply formula (5) to function

$$x\left(t'\right) = \cos\left(\omega_c t' + \varphi\left(t'\right)\right) \cdot \cos\left(\omega_c t'\right).$$ (6)

Suppose that function $\varphi\left(t'\right)$ can be expanded in a Taylor series near point $t' = t$. Let us take two terms of this series on the segment $t + T_c \geq t' \geq t$

$$\varphi\left(t'\right) \approx \varphi\left(t\right) + \dot{\varphi}\left(t\right) \cdot \left(t' - t\right),$$

where $\dot{\varphi}\left(t\right)$ denotes the derivative.

The function slowly changes over this interval. Integral (5) is approximately calculated

$$y\left(t\right) = \frac{1}{T_c} \cdot \int\limits_t^{t+T_c} \cos\left(\omega_c \cdot t' + \varphi\left(t'\right)\right) \cdot \cos\left(\omega_c \cdot t'\right) dt'$$

$$\approx \frac{1}{T_c} \cdot \int\limits_t^{t+T_c} \cos\left(\left(\omega_c + \dot{\varphi}\left(t\right)\right) \cdot t' + \varphi\left(t\right) - \dot{\varphi}\left(t\right) \cdot t\right) \cdot \cos\left(\omega_c \cdot t'\right) dt'.$$

The integral is as follows

$$y\left(t\right) = \frac{1}{T_c} \sin\left(\dot{\varphi}\left(t\right) \frac{T_c}{2}\right) \left(\frac{\cos\left(\varphi\left(t\right) + \dot{\varphi}\left(t\right) \frac{T_c}{2}\right)}{\dot{\varphi}\left(t\right)} + \frac{\cos\left(\left(2\omega_c t + \varphi\left(t\right) + \dot{\varphi}\left(t\right) \frac{T_c}{2}\right)\right)}{2\omega_c + \dot{\varphi}\left(t\right)}\right).$$ (7)

Assuming that $\dot{\varphi}\left(t\right) T_c/2 \ll 1$, we obtain the approximate solution

$$y\left(t\right) \approx \frac{1}{2} \cos\left(\varphi\left(t\right) + \dot{\varphi}\left(t\right) \frac{T_c}{2}\right) + \frac{\dot{\varphi}\left(t\right)}{4\omega_c} \cos\left(2\omega_c t + \varphi\left(t\right) + \dot{\varphi}\left(t\right) \frac{T_c}{2}\right).$$ (8)

Formula (8) provides a first-order correction for the rate of phase change $\varphi\left(t\right)$ to the result of averaging the function (6), obtained using formula (5). It is easy to show that the discrete version of the moving average filter formula (3) gives a similar formula for the averaging correction. Therefore, further corrections to the signals will be calculated using simple formula (5).

4. Signals correction

Let's find corrections to signals $S\left(t\right)$, $C\left(t\right)$ with using formula of moving average filter in continuous form. By definition, signals $S\left(t\right)$, $C\left(t\right)$ are calculated by formulas (with using LP moving average filter)

$$C\left(t\right) = \frac{1}{T_c} \cdot \int\limits_t^{t+T_c} \frac{S_{in}\left(t'\right)}{G} \cdot \cos\left(\omega_c t'\right) dt',$$

$$S\left(t\right) = \frac{1}{T_c} \cdot \int\limits_t^{t+T_c} \frac{S_{in}\left(t'\right)}{G} \cdot \sin\left(\omega_c t'\right) dt'.$$

After substitution of (2), one obtains

$$C\left(t\right) = \frac{1}{T_c} \cdot \int\limits_t^{t+T_c} \cos\left(\text{Saw}\left(t'\right) + \varphi\left(t'\right)\right) \cdot \cos\left(\omega_c t'\right) dt',$$

$$S\left(t\right) = \frac{1}{T_c} \cdot \int\limits_t^{t+T_c} \cos\left(\text{Saw}\left(t'\right) + \varphi\left(t'\right)\right) \cdot \sin\left(\omega_c t'\right) dt'.$$

The time axis is divided into intervals of width T_c. Let's say that selected random moment of time t' belongs to interval with number k, so that moment t' is located in interval $kT_c \leq t' \leq \left(k+1\right) T_c$. Moment $t' + T_c$ is located in interval $\left(k+1\right) T_c < t' \leq \left(k+2\right) T_c$. Sawtooth curve $\text{Saw}\left(t'\right)$ is as follows:

$$\text{Saw}\left(t'\right) = \begin{cases} \Omega \cdot \left(t' - kT_c\right), & kT_c \leq t' \leq \left(k+1\right) T_c; \\ \Omega \cdot \left(t' - \left(k+1\right) T_c\right), & \left(k+1\right) T_c < t' \leq \left(k+2\right) T_c. \end{cases}$$ (9)

Substitution of (9) into integrals for $S(t)$, $C(t)$ gives one the following expressions:

$$C(t) = \frac{1}{T_c} \cdot \int_t^{(k+1)T_c} \cos\left(\Omega \cdot (t' - kT_c) + \varphi(t')\right) \cdot \cos\left(\omega_c t'\right) dt'$$

$$+ \frac{1}{T_c} \cdot \int_{(k+1)T_c}^{t+T_c} \cos\left(\Omega \cdot (t' - kT_c) + \varphi(t')\right) \cdot \cos\left(\omega_c t'\right) dt',$$

$$S(t) = \frac{1}{T_c} \cdot \int_t^{(k+1)T_c} \cos\left(\Omega \cdot (t' - kT_c) + \varphi(t')\right) \cdot \sin\left(\omega_c t'\right) dt'$$

$$+ \frac{1}{T_c} \cdot \int_{(k+1)T_c}^{t+T_c} \cos\left(\Omega \cdot (t' - kT_c) + \varphi(t')\right) \cdot \sin\left(\omega_c t'\right) dt'.$$

Suppose that angle of "saw" differs little from ω_c

$$\Omega = \omega_c - \Delta, \quad |\Delta| \ll \omega_c.$$

Phase $\varphi(t')$ changes slowly enough (doesn't exceed dynamic range), so $\dot{\varphi}(t) \ll \omega_c$. Let's introduce infinitesimal order:

$$\zeta = \frac{\Delta}{\omega_c}, \quad \xi = \frac{\dot{\varphi}(t)}{\omega_c}.$$

Let us find functions $S(t)$, $C(t)$ with first order accuracy in parameters ζ, ξ. One can write

$$S(t) = S^{(0)}(t) + \delta_s(t),$$
$$C(t) = C^{(0)}(t) + \delta_c(t)$$

and obtain

$$S^{(0)}(t) = -\frac{1}{2}\sin\left(\varphi(t)\right),$$

$$C^{(0)}(t) = \frac{1}{2}\cos\left(\varphi(t)\right),$$

$$\delta_s(t) = -\frac{1}{4}\zeta \cdot \sin\left(\varphi(t)\right) + \frac{\pi}{2}(\zeta - \xi) \cdot \cos\left(\varphi(t)\right) + \frac{1}{4}\xi \cdot \sin\left(2\omega_c t + \varphi(t)\right),$$

$$\delta_c(t) = -\frac{1}{4}\zeta \cdot \cos\left(\varphi(t)\right) + \frac{\pi}{2}(\zeta - \xi) \cdot \sin\left(\varphi(t)\right) + \frac{1}{4}\xi \cdot \cos\left(2\omega_c t + \varphi(t)\right).$$

5. ATAN-method of phase calculation $\varphi(t)$ and results

Phase $\varphi(t)$ calculation is made with arctangent function in the IQ protocol. Due to the filtering error, the calculated phase $\tilde{\varphi}(t)$ will be distorted. Let's find excited phase within the first order of ξ, ζ parameters:

$$\tilde{\varphi}(t) = \arctan\left(\frac{-S(t)}{C(t)}\right) = \arctan\left(\frac{\sin\left(\varphi(t)\right)}{\cos\left(\varphi(t)\right)}(1 - \gamma(t))\right),$$

$$\gamma(t) = 2\frac{\delta_c(t)}{\cos\left(\varphi(t)\right)} + 2\frac{\delta_s(t)}{\sin\left(\varphi(t)\right)}.$$

Finally, phase with LPF errors is calculated as follows:

$$\tilde{\varphi}(t) = \varphi(t) - \pi(\zeta - \xi) + \frac{1}{2}\zeta \cdot \sin\left(2\varphi(t)\right) - \frac{1}{2}\xi \cdot \sin\left(2\omega_c t + 2\varphi(t)\right). \tag{10}$$

Let's determine the theoretical correction to the calculated phase

$$\Delta\Phi_{\text{teor}}(t) = \tilde{\varphi}(t) - \varphi(t). \tag{11}$$

Now we need to perform mathematical modeling of the IQ demodulation algorithm. Let us choose the phase change function as follows:

$$\varphi(t) = \pi\left(\cos\left(0.05 \cdot \nu_c \cdot t\right) - 1\right),$$
$$\nu_c = \frac{\omega_c}{2\pi} = 2 \cdot 10^4, \, \text{s}^{-1}. \tag{12}$$

Select the sampling step Δt, which is equal to the sampling period:

$$\Delta t = T_d = 5 \cdot 10^{-7}, \, \text{s}.$$

Modelling steps are as follows:

1. Input signal (2) is multiplied by two harmonics: $\cos(\omega_c t)$ and $\sin(\omega_c t)$, which gives one the following functions:

$$FC(t) = \cos(\text{Saw}(t) + \varphi(t)) \cdot \cos(\omega_c t),$$
$$FS(t) = \cos(\text{Saw}(t) + \varphi(t)) \cdot \sin(\omega_c t).$$

2. These functions are discretized:

$$FC_p = FC(\Delta t \cdot p),$$
$$FS_p = FS(\Delta t \cdot p).$$

3. The resulting vectors are filtered using the moving average method:

$$C_n = \frac{1}{P} \cdot \sum_{j=n}^{n+P-1} FC_j,$$

$$S_n = \frac{1}{P} \cdot \sum_{j=n}^{n+P-1} FS_j.$$

4. Next, we applied the ATAN procedure allowing us phase calculation, which values are continuously extended from the range of arctangent function to the whole axis. The result is the distorted phase $\tilde{\tilde{\varphi}}_n$, found in discretization points:

$$\tilde{\tilde{\varphi}}_n = \arctan\left(-\frac{S_n}{C_n}\right).$$

5. Let us introduce the notation for the experimental correction

$$\Delta\Phi_{\text{exp}}(t) = \tilde{\tilde{\varphi}}_n - \varphi(\Delta t \cdot n). \tag{13}$$

and compare graphically $\Delta\Phi_{\text{teor}}(t)$ and $\Delta\Phi_{\text{exp}}(t)$.

Figure 1 shows "saw" graph with taking into account the form error ζ, $\zeta = 0.1$. A study of the thermal modulation process of VCSEL wavelength is presented in paper [21] for the case of periodic sinusoidal modulation.

For chosen $\varphi(t)$ (12) the maximum parameter ξ is

$$\xi_{\text{max}} = 0.025.$$

Figure 2 demonstrates error in phase determining found by the method of mathematical modeling and the error in phase determining, calculated using formula (10). One can see that the result of mathematical modelling of phase errors and the result of analytical phase errors calculation is almost identical.
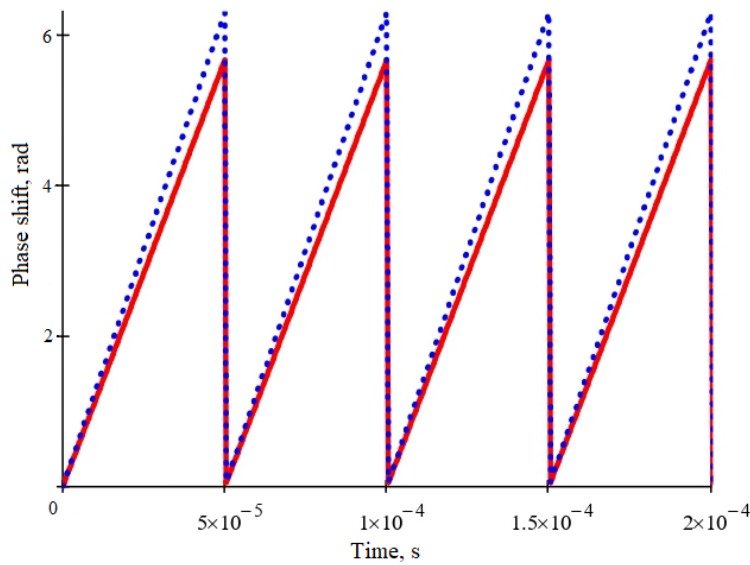

FIG. 1. VCSEL sawtooth phase modulation. Solid line – distorted saw with incline Ω (9), dotted line – ideal saw with incline ω_c.
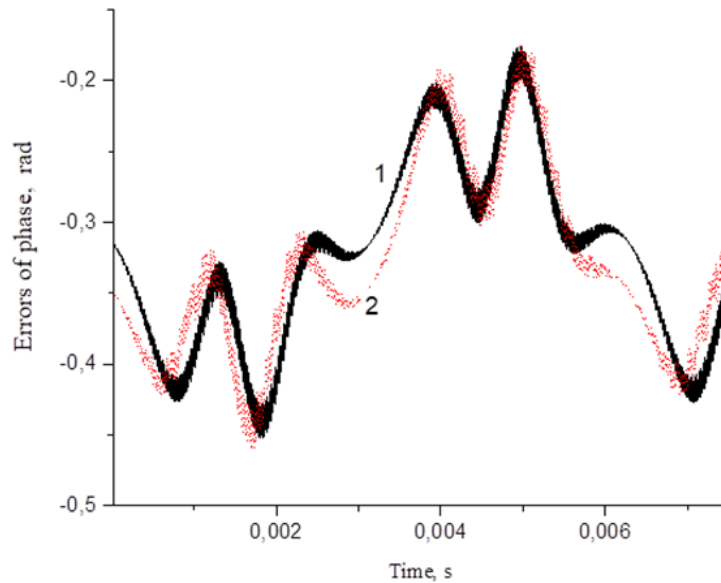
FIG. 2. Phase errors, 1 – analytically calculated error $\Delta\Phi_{\text{teor}}(t)$ (11), 2 – experimentally calculated error $\Delta\Phi_{\text{exp}}(t)$ (13)

6. Conclusion

This article is devoted to the study of errors that arise in the demodulated phase due to the passage of the processed signal through a low-pass filter in the IQ algorithm. In this work, we considered a signal with sawtooth wavelength modulation, which has its own form errors which further distorts the signal supplied to the demodulation circuit. Taking into account the saw shape error, as well as taking into account the calculated phase corrections due to the influence of the moving average filter, an adjusted formula for the signal was obtained, which is fed to the IQ processing circuit. To confirm the calculations, mathematical modeling was carried out using experimentally obtained parameters. It is shown that the results of modeling and analytical solutions correlate well with each other. This work will improve the quadrature demodulation method, which will allow better processing of data from interferometric sensors using VCSEL as a source.

References

[1] Li Y., et al. Phase Demodulation Methods for Optical Fiber Vibration Sensing System: A Review. *IEEE Sensors J.*, 2022, **22** (3), P. 1842–1866.

[2] Guojie Tu, Benli Yu, Mengmeng Zhao, Jiping Lin. A phase-sensitive optical time-domain reflectometry system with an electrical I/Q demodulator. *Proceedings of the SPIE 10821, Advanced Sensor Systems and Applications VIII*, 2018, 1082123.

[3] Hartog A., Frignet B., Mackie D., Clark M. Vertical seismic optical profiling on wireline logging cable. *Geophysical Prospecting*, 2014, **62**, P. 693–701.

[4] He X., et al. Multi-event waveform-retrieved distributed optical fiber acoustic sensor using dual-pulse heterodyne phase-sensitive OTDR. *Optics Letters*, 2017, **42**, P. 442–445.

[5] Yu M., Liu M., Chang T., Lang J., Chen J., Cui H.-L. Phase-sensitive optical time-domain reflectometric system based on a single-source dual heterodyne detection scheme. *Applied Optics*, 2017, **56**, P. 4058–4064.

[6] Lu Y., Zhu T., Chen L., Bao X. Distributed vibration sensor based on coherent detection of phase-OTDR. *J. of Lightwave Technology*, 2010, **28** (22), P. 3243–3249.

[7] Pan Z., Liang K., Ye Q., Cai H., Qu R., Fang Z. Phase-sensitive OTDR system based on digital coherent detection. *Optical Sensors and Biophotonics, Proceedings of the SPIE 8311 (Optical Society of America)*, 2011, 83110S.

[8] Yuelan Lu, Tao Zhu, Liang Chen, Xiaoyi Bao. Distributed Vibration Sensor Based on Coherent Detection of Phase-OTDR. *J. of Lightwave Technology*, 2010, **28** (22), 3243.

[9] Yongkang Dong, Xi Chen, Erhu Liu, Cheng Fu, Hongying Zhang, Zhiwei Lu. Quantitative measurement of dynamic nanostrain based on a phase-sensitive optical time domain Reflectometer. *Applied Optics*, 2016, **55** (28), P. 7810–7815.

[10] Qin M., He X., Liu F., Zheng X., Zhang M. Real-time phase demodulation and data administration of distributed optical fiber vibration sensing system. *Proceedings of the SPIE*, 2017, **10208**, P. 1020810–1020818.

[11] Zinan Wang, Li Zhang, Song Wang, Naitian Xue, Fei Peng, Mengqiu Fan, Wei Sun, Xianyang Qian, Jiarui Rao, Yunjiang Rao. Coherent Φ-OTDR based on I/Q demodulation and homodyne detection. *Optics Express*, 2016, **24** (2), P. 853–858.

[12] Martins H.F., Shi K., Thomsen B.C., Martin-Lopez S., Gonzalez-Herraez M., Savory S.J. Real time dynamic strain monitoring of optical links using the backreflection of live PSK data. *Optics Express*, 2016, **24** (19), P. 22303–22318.

[13] Yan Q., Tian M., Li X., Yang Q., Xu Y. Coherent Φ-OTDR based on polarization-diversity integrated coherent receiver and heterodyne detection. *Proceedings of the SPIE*, 2017, **10323**, P. 1032383–1032386.

[14] Fang G., Xu T., Li F. Heterodyne interrogation system for TDM interferometric fiber optic sensors array. *Optics Communications*, 2015, **341**, P. 74–78.

[15] Song M., Yin S., Ruffin P.B. Fiber Bragg grating strain sensor demodulation with quadrature sampling of a Mach–Zehnder interferometer. *Applied Optics*, 2000, **39** (7), P. 1106–1111.

[16] Fu Y., Xue N., Wang Z., Zhang B., Xiong J., Rao Y. Impact of I/Q amplitude imbalance on coherent – OTDR. *J. of Lightwave Technology*, 2018, **36** (4), P. 1069–1075.

[17] Faruk M.S., Kikuchi K. Compensation for In-Phase/Quadrature imbalance in coherent-receiver front end for optical quadrature amplitude modulation. *IEEE Photonics J.*, 2013, **5** (2), 7800110.

[18] Chang S.H., Chung H.S., Kim K. Impact of quadrature imbalance in optical coherent QPSK receiver. *IEEE Photonics Technology Letters*, 2009, **21** (11), P. 709–711.

[19] Naitian Xue, Yun Fu, Chongyu Lu, Ji Xiong, Le Yang, Zinan Wang. Characterization and Compensation of Phase Offset in Φ-OTDR with Heterodyne Detection. *J. of Lightwave Technology*, 2018, **36** (23), P. 5481–5487.

[20] Miroshnichenko G.P., Arzhanenkova A.N., Plotnikov M.Y. Errors in the demodulation algorithm with a generated carrier phase introduced by the low-pass filter. *Scientific and Technical J. of Information Technologies, Mechanics and Optics*, 2023, **23** (4), P. 795–802 (in Russian).

[21] Miroshnichenko G.P., Arzhanenkova A.N., Plotnikov M.Y. Investigation of the method of current thermal modulation of the wavelength VCSEL. *Nanosystems: Physics, Chemistry, Mathematics*, 2022, **13** (6), P. 615–620.

Information about the authors:

George P. Miroshnichenko – Research Center of light guide photonics, ITMO University, Kronverksky pr. 49, St. Petersburg, 197101, Russia; ORCID 0000-0002-4265-8818; gpmirosh@gmail.com

Alina N. Arzhanenkova – Research Center of light guide photonics, ITMO University, Kronverksky pr. 49, St. Petersburg, 197101, Russia; ORCID 0000-0003-4869-2838; 11arzh11@gmail.com

Michail Yu.Plotnikov – Research Center of light guide photonics, ITMO University, Kronverksky pr. 49, St. Petersburg, 197101, Russia; ORCID 0000-0003-2506-0379; plotnikov-michael@yandex.ru

Conflict of interest: the authors declare no conflict of interest.